One-Pot Synthesis of Hairy Nanoparticles by Emulsion ATRP

Ke Min, Haifeng Gao, Jeong Ae Yoon, Wei Wu, Tomasz Kowalewski, and Krzysztof Matyjaszewski*

Department of Chemistry, Carnegie Mellon University, 4400 Fifth Avenue, Pittsburgh, Pennsylvania 15213

Received November 22, 2008; Revised Manuscript Received December 31, 2008

ABSTRACT: An efficient one-pot synthesis of hairy nanoparticles was developed by applying ATRP to a two-step sequential emulsion copolymerization. The first step was a microemulsion ATRP of methyl methacrylate (MMA) monomer and ethylene glycol dimethacrylate (EGDMA) cross-linker, leading to uniform nanogels with hydrodynamic diameter $D_h = 31$ nm, determined by dynamic light scattering measurement. Addition of a second monomer, *n*-butyl acrylate (*n*BA), to the microemulsion successfully converted the system into an emulsion polymerization, and linear P*n*BA arms grew from the retained initiating sites in the nanogels, forming hairy nanoparticles in situ. The use of an emulsion medium allowed the preparation of hairy nanoparticles with uniform size (coefficient of variation <0.3), and the particle size increased from $D_h = 38$ to 100 nm with the increasing *n*BA conversion. Based on the GPC analyses of the cleaved products of nanogel cores and hairy nanoparticles containing degradable disulfide cross-link, the number of grafted polymer chains per hairy nanoparticle was estimated to be $N_{hair} \sim 2.3 \times 10^3$, corresponding to a maximum grafting density of 0.75 chains/nm^2 on the surface of nanogel. Direct visualization of the hairy nanoparticles by atomic force microscopy provided additional evidence for the successful synthesis of uniform-sized particles.

Introduction

Among the various topologies that can be attained from polymeric nanoparticles, hairy nanoparticles are of particular interest. They have a core−shell structure in which the shell is composed of linear polymer chains with high affinity to the dispersion medium. Because of their small size and the presence of multiple functionalities on shell periphery,[1] these hairy nanoparticles readily find use in biochemical diagnostics and as stimuli-responsive materials.[2−4] Moreover, they are important materials for enhancing the mechanical properties of thermoplastics and formation of scratch-resistant coatings due to the properties provided by the relatively rigid core and flexible hairy shell.[5,6]

Hairy nanoparticles include particles containing either an inorganic core or a polymeric core. In the latter case, the hairy nanoparticles are usually synthesized by grafting linear polymer chains from,[7,8] or onto,[9] existing nanogel particles that are generally defined as internally cross-linked single macromolecules with a number of transverse covalent bonds between the chain segments.[10] Compared to the "grafting onto" process, the "grafting from" method results in a higher grafting density on the particle surface and could therefore be the favored synthetic method.[11] Evidently, the development of controlled/"living" radical polymerization (CRP)[12,13] techniques provides additional advantages for "grafting from" method and has been frequently employed for the preparation of hairy nanoparticles.[1,14−20]

A "two-pot" synthesis is generally required for the synthesis of hairy particles, i.e., (a) the synthesis, isolation, and purification of the nanogel particles and (b) the synthesis of hairs, or grafted linear chains, from the particle surface. Recently, a convenient "one-pot" synthetic route has been reported which involves growing chains from an in situ generated nanogel core using CRP techniques.[21−23] The nanogel core was synthesized by copolymerization of monovinyl monomer and divinyl cross-linker. The cross-linker was mostly consumed before the second batch of monovinyl monomer was added to grow polymer chains from the retained initiating sites in the nanogel in a divergent fashion, forming a hairy nanoparticle. The size of the hairy nanoparticle can be adjusted by changing the concentrations and ratios of monomer/cross-linker in the initial system that forms the core and the degree of polymerization (DP) of the linear polymers forming the "hairy" shell. Therefore, this one-pot procedure provides a simple method for the synthesis of hairy nanoparticles with no need for purification of intermediates.

The most important requirement, in this seemingly convenient synthetic route, is to synthesize the parent nanogel core in a dilute system in order to prevent macroscopic gelation by suppressing intermolecular cross-linking reactions.[21,24] However, it is difficult to completely avoid interactions between the individual nanogels in a homogeneous solution and exercise control over the size of the nanogels. Consequently, the resulting hairy nanoparticles display a broad size distribution (or broad molecular weight distribution) due to this limited control over the particle size in the first step.[23]

Conducting a polymerization in an emulsion medium is a widely known procedure that provides a route for the synthesis of uniform nanoparticles.[25,26] In the present study, we report the synthesis of hairy nanoparticles by using atom transfer radical polymerization (ATRP)[27−30] in an emulsion system[31,32] (Scheme 1). A polymeric nanogel core was first synthesized by activators generated by electron transfer (AGET)[33,34] ATRP of a monovinyl monomer and a divinyl cross-linker in a microemulsion,[35] where uniform latex was obtained and each microemulsion particle consisted of one parent nanogel. The microemulsion latexes were employed as seeds for an emulsion polymerization during the second step, by the addition of another monovinyl monomer that polymerized from the nanogel core and formed linear polymeric hairs. Since the first copolymerization/cross-linking step occurred inside a single, well-defined microemulsion particle, the parent nanogels possessed narrow size distribution before additional monomer was added to the ongoing polymerization for hair growth. This procedure retained the advantage of a one-pot synthesis, i.e., no need to isolate or purify any intermediate material, and resulted in the synthesis of uniform hairy nanoparticles.

* Corresponding author. E-mail: km3b@andrew.cmu.edu.

10.1021/ma8026244 CCC: $40.75
Published on Web 02/03/2009

Scheme 1. One-Pot Synthesis of Hairy Nanoparticles by ATRP in Emulsion

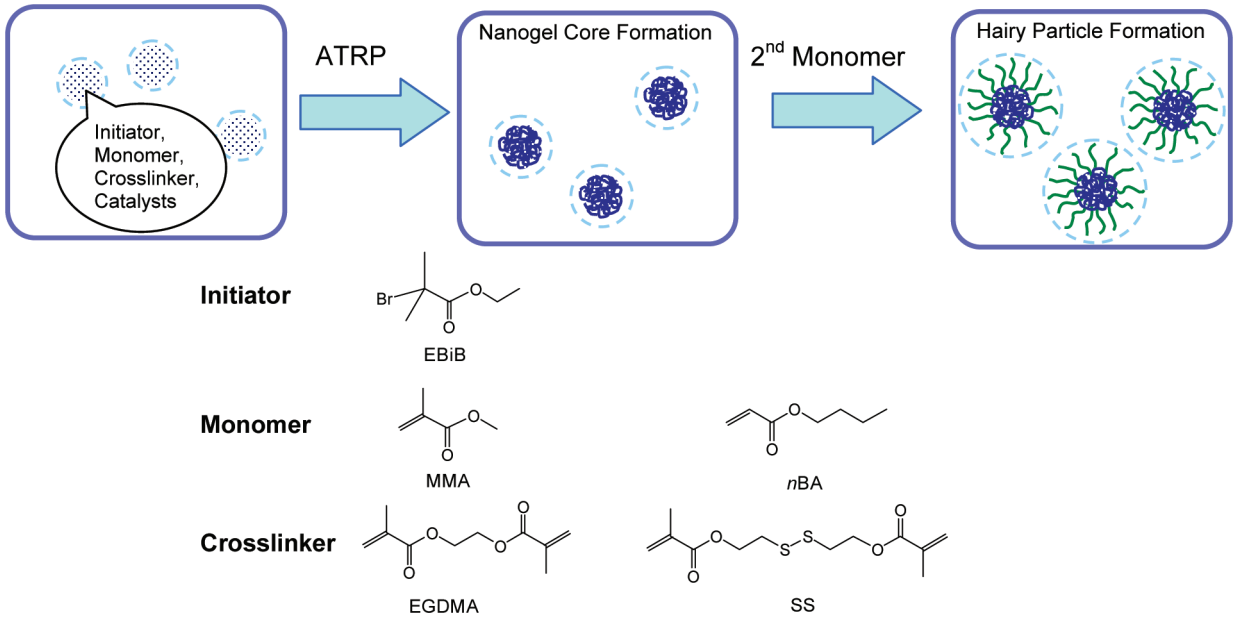

Experimental Section

Materials. All chemicals, including (polyoxyethylene(20) oleyl ether) (Brij 98), ethyl 2-bromoisobutyrate (EBiB), and tri-*n*-butylphosphine (Bu_3P), were purchased from Aldrich and were used as received unless otherwise stated. Methyl methacrylate (MMA, 99%), ethylene glycol dimethacrylate (EGDMA, 98%), and *n*-butyl acrylate (*n*BA, 98%) were purified by passing through a column filled with basic alumina (Sorbent technologies) to remove inhibitor and/or antioxidant and were stored at −5 °C. Bis(2-pyridylmethyl)-octadecylamine (BPMODA) was synthesized according to the previously published procedure.[36] The degradable cross-linker, bis(methacryloyloxyethyl) disulfide (SS), was synthesized using a literature procedure.[37]

Synthesis of PMMA−P*n*BA Hairy Nanoparticles in Emulsion. Before conducting a microemulsion polymerization, the Cu(II) complex was prepared by dissolving $CuBr_2$ and BPMODA in MMA at 60 °C. After dissolving EBiB initiator and EGDMA cross-linker in this solution, the resulting mixture was slowly injected into a flask containing an aqueous solution of Brij 98 at 60 °C to form a transparent microemulsion. The microemulsion was purged with nitrogen for 30 min, before the flask was immersed in an oil bath thermostated at 65 °C. An aqueous solution of ascorbic acid was injected into the reaction to activate the catalyst complex and initiate the polymerization.[35] The magnetic stirring rate remained at ∼100 rpm throughout the microemulsion polymerization. At the time of 1.2 h after initiation of microemulsion ATRP, the deoxygenated *n*BA monomer was added to the microemulsion polymerization, converting the microemulsion to a seeded emulsion system (this moment was recorded as $t = 0$ for *n*BA). After the addition of *n*BA, the polymerization temperature was increased to 80 °C, while the magnetic stirring rate remained at ∼100 rpm for another 6 h in order to maintain the emulsion stability. After that, the stirring rate was increased to 600 rpm until the polymerization was stopped by exposing the system to air. The stoichiometry of reagents used in the experiment is listed in Table 1.

Characterization. Monomer conversion was measured gravimetrically. The dried samples were dissolved in THF and filtrated through 220 nm filters before they were subjected to gel permeation chromatography (GPC) analysis (Polymer Standards Services (PSS) columns (guard, 10^5, 10^3, and 10^2 Å), with THF eluent at 35 °C, flow rate = 1.00 mL/min, and differential refractive index (RI) detector (Waters, 2410)). The apparent molecular weight and polydispersity (M_w/M_n) of each sample were determined with a calibration based on linear polystyrene (PSt) standards using WinGPC 6.0 software from PSS. Area fractions of different polymer species in one GPC curve were determined by multipeak splitting of the GPC curve using Gaussian function in Origin 6.0 software. The detectors employed to measure the absolute molecular weights ($M_{w,MALLS}$) were a triple detector system containing RI detector (Wyatt Technology, Optilab REX), viscometer detector (Wyatt Technology, ViscoStar), and a multiangle laser light scattering (MALLS) detector (Wyatt Technology, DAWN EOS) with the light wavelength at 690 nm. Absolute molecular weights were determined using ASTRA software from Wyatt Technology. The latex samples were directly taken from the reaction and diluted with deionized water by a factor of 5 before they were subjected to the latex size and size distribution measurement by dynamic light scattering (DLS) at 25 °C on a high performance particle sizer, model HP5001 from Malvern Instruments, Ltd. The samples were dried and washed with methanol to remove surfactants and then redispersed in THF (concentration ∼1 mg/mL) at room temperature for a second particle size measurement.

Table 1. One-Pot Synthesis of Hairy Nanoparticles PMMA−P*n*BA[a]

		molar ratio	weight (g)
core	MMA	18	0.3927
	EBiB	1	0.0425
	$CuBr_2$/BPMODA	0.15/0.15	0.0073/0.0147
	Brij98		0.9
	H_2O		24
	ascorbic acid	0.0375	0.0015
	EGDMA	2	0.0864
shell	*n*BA	150	4.1940

[a] Polymerization temperature for core formation: 65 °C; polymerization temperature for shell growth: 80 °C.

In order to conduct AFM characterization, the polymer nanoparticles were suspended in chloroform (0.2 mg/mL) and spin-casted onto freshly cleaved mica surfaces at 4000 rpm. The samples were then dried under ambient conditions overnight. Tapping mode AFM experiments were carried out using a Multimode Nanoscope III system (Digital Instruments, Santa Barbara, CA). The measurements were performed in air using commercial Si cantilevers with a nominal spring constant and resonance frequency respectively equal to 5 N/m and 130 kHz. The height and phase images were acquired simultaneously at set-point ratio $A/A_0 = 0.8-0.9$, where A and A_0 refer to the "tapping" and "free" cantilever amplitude, respectively. The free cantilever amplitude was targeted to 2 V due to the stickiness of P*n*BA chains. The AFM images were rendered using

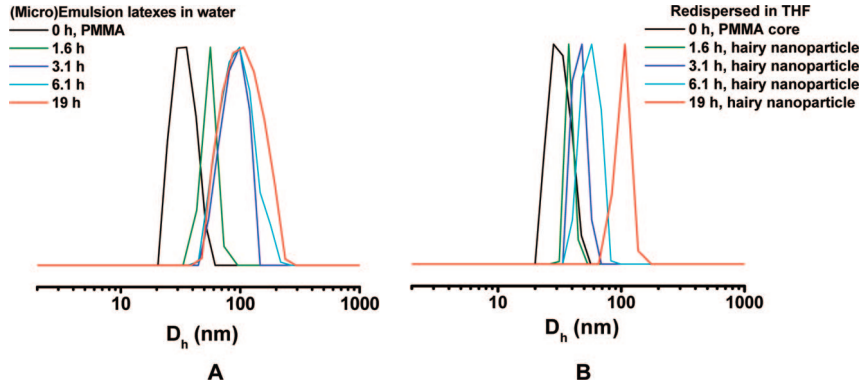

Figure 1. Hydrodynamic size distribution of (A) the (micro)emulsion latexes in water and (B) the obtained nanoparticles in THF, measured by DLS at room temperature. For aqueous measurement, the latex samples were directly taken from the reaction and diluted with deionized water by a factor of 5. The samples were dried and washed with methanol to remove surfactants before redispersed in THF (concentration ~1 mg/mL) for a further measurement.

Table 2. Particle Size and Molecular Weight during the One-Pot Synthesis of Hairy Nanoparticles by ATRP in Emulsion[a]

time (h, for *n*BA)[b]	conversion (%, for *n*BA)	D_h (nm, in water)	D_h (nm, in THF)	$M_{w,RI}$ (g/mol)[c]	$M_{w,MALLS}$ (g/mol)[d]	$M_{w,MALLS}/M_{w,RI}$
0	0.0	31	31	1.41×10^5	5.50×10^6	39.1
1.6	5.1	55	38	1.77×10^5	7.10×10^6	40.1
3.1	12	80	45	2.68×10^5	9.20×10^6	34.4
6.1	20	91	55	3.73×10^5	1.11×10^7	29.8
19	60	97	100	1.38×10^6	2.50×10^7	18.1

[a] Polymerization conditions: see Table 1. [b] Polymerization time after the addition of 150 equiv of *n*BA. [c] $M_{w,RI}$ represents the apparent weight-average molecular weight obtained from THF GPC with RI detector, based on linear PSt standard. [d] $M_{w,MALLS}$ represents the absolute weight-average molecular weight obtained from THF GPC equipped with MALLS detectors.

the custom software written in MATLAB 7.5 (The MathWorks Inc., Natick, MA).

Thermal behavior of the hairy nanoparticles was measured by differential scanning calorimeter (DSC, TA Instruments DSC-Q 100) at a heating rate of 10 °C/min under a nitrogen atmosphere over a temperature range of −60 to 180 °C. The second heating cycle was recorded.

Results and Discussion

Synthesis of Hairy Nanoparticles Using ATRP in an Emulsion System. Emulsion polymerization is a commonly used method for preparation of uniform polymeric nanoparticles.[25] Recently, ATRP has been successfully adapted to the rigors of an emulsion system providing well-defined polymers by using a continuous two-step procedure, in which a seeded emulsion was formed by adding pure monomer to an ongoing microemulsion ATRP.[38] This procedure avoids the need to transport catalysts through the aqueous media during the polymerization and therefore facilitates a controlled ATRP in the active latexes. One advantage of carrying out ATRP in microemulsion, or emulsion, is that the chain-end functionalities of the polymer chains are retained in each latex particle. This makes it easy to subsequently perform chain extension and/or particle surface modification if the (micro)emulsion polymerization is applied for a particle synthesis.[20,39]

In the present approach to prepare hairy nanoparticles, the initial synthesis of cross-linked PMMA nanoparticles was carried out by conducting a microemulsion ATRP of MMA and divinyl cross-linker EGDMA. The nanogel was formed inside the microemulsion latex, and therefore the size of the nanogel closely resembled the size of the latex. A high polymerization rate was achieved within the microemulsion latexes by selecting a low targeted $DP_{target} = 22$, e.g., $[MMA]_0:[EGDMA]_0:[EBiB]_0 = 18:2:1$. The conversion of MMA reached essentially 100% at 1.2 h after initiation of the microemulsion ATRP, and then a second batch of monomer, *n*BA, was fed to the microemulsion polymerization system. Since all initiating sites were retained within the microemulsion latexes, the only option for the added

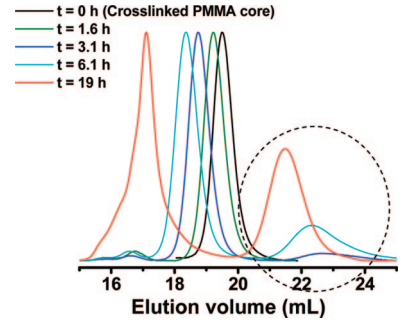

Figure 2. GPC traces (RI detector) of the polymers (nanoparticles) obtained from ATRP in emulsion, with THF as eluent and linear PS as standard. The peaks circled by a dashed ellipse represent linear polymers. Polymerization conditions: see Table 1.

*n*BA to polymerize was to diffuse into each active latex and participate in a "grafting from" polymerization.[38] The polymer chains grew from the accessible chain-end functionalities within the cross-linked nanogel and formed a hairy shell tethered to the nanogel core. Thus, a hairy nanoparticle (or a starlike structure[23]) was obtained.

The nanogels and hairy nanoparticles at different times were subjected to DLS analysis for measurement of particle size, i.e., hydrodynamic diameter (D_h). As seen in Figure 1A, the size of the latex particles steadily increased from $D_h = 31$ nm ($t = 0$ h, the moment when *n*BA was added) to $D_h = 97$ nm ($t = 19$ h) as the conversion of *n*BA reached 60% (Table 2). During the entire polymerization, the size distribution of the microemulsion/emulsion latex particles remained narrow with coefficient of variation <0.3.

The latex samples were dried and washed with methanol to remove the surfactants before they were dissolved in THF for an additional DLS measurement of the hairy nanoparticles. The results in Figure 1B and Table 2 show that the hydrodynamic diameter of the hairy nanoparticles in THF was smaller than that of the corresponding latexes in water because the residual

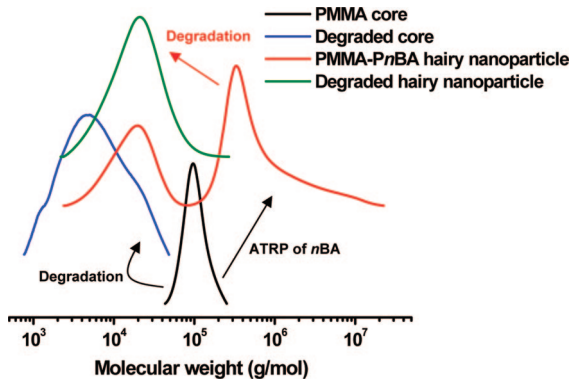

Figure 3. GPC traces of nanogel core, hairy nanoparticle before and after degradation upon addition of Bu_3P, with THF as eluent and linear PSt as standard. The nanogel was synthesized by ATRP of MMA and SS ($[MMA]_0:[SS]_0:[EBiB]_0 = 18:2:1$) in microemulsion and hairy nanoparticle was obtained by in situ chain extension of *n*BA from the nanogel in emulsion ($DP_{nBA,target} = 200$).

unreacted monomers in the emulsion latexes were removed before DLS analysis of the hairy nanoparticles in THF. In addition, during the DLS analysis in THF, the fact that some low-molecular-weight linear polymer chains diffused out of the nanoparticles to THF solution also contributed to the size discrepancy. Nevertheless, at higher *n*BA conversion, e.g., 60%, the size of the nanoparticles was very close to that of the emulsion latexes, suggesting that essentially one hairy nanoparticle was formed within each emulsion latex.

The THF-dispersed nanogels were subjected to the molecular weight analysis by GPC. Both nanogel cores and the hairy nanoparticles displayed an apparent narrow molecular weight distribution (MWD, $M_w/M_n = 1.1-1.3$) (Figure 2). This result confirms the advantage of the procedure, a continuous microemulsion/seeded emulsion ATRP, for preparation of uniform nanoparticles with retained chain-end functionalities. After chain extension via polymerization of *n*BA, the GPC traces in Figure 2 show two elution peaks, representing the obtained hairy nanoparticles and a fraction of linear polymers (a peak at higher elution volume, circled by a dashed ellipse). Both peaks shifted toward higher molecular weight with the increase of *n*BA conversion, indicating the "livingness" of the polymers that formed in the initial microemulsion ATRP. The low-molecular-weight linear polymers represented the product of the chain extension of linear PMMA chains that were not bound to the nanogel cores. The hairy nanoparticles could be easily separated from these linear polymers by several methods, such as centrifugation, selective precipitation, and fractionation using preparative GPC columns.

It is anticipated that the compactness of the hairy nanoparticles should decrease with polymerization time because of the growth of the loose hairy shell, as compared to the rigid cross-linked nanogel core. The structural compactness of the hairy nanoparticles can be evaluated by the ratio of absolute molecular weight (measured by GPC with MALLS detector) and apparent molecular weight (measured by THF GPC with a RI detector using linear PSt standards).[40] In GPC MALLS measurement, the d*n*/d*c* value of each sample in THF was calculated based on the weight fraction of PMMA (d*n*/d*c* = 0.088 mL/g in THF) and P*n*BA (d*n*/d*c* = 0.069 mL/g in THF)[41] in the sample, obtained from monomer conversion data. The absolute weight-average molecular weight of the PMMA−P*n*BA hairy nanoparticles at 19 h was $M_{w,MALLS} = 2.50 \times 10^7$ g/mol, which is 18.1 times higher than the apparent molecular weight, $M_{w,RI} = 1.38 \times 10^6$ g/mol (Table 2). The significant difference between the values of $M_{w,MALLS}$ and $M_{w,RI}$ indicates a highly compact structure of the hairy nanoparticles. The ratio of $M_{w,MALLS}$ to $M_{w,RI}$ in Table 2 decreased as the conversion of *n*BA increased, indicating a loosening structure as the hairy polymer chains grew from the surface of the core. This combination of hard core and soft shell might suggest application of the hairy nanoparticles as a component of mechanically enhanced composite materials.

Evaluation of Number-Average Number of Grafted Chains per Hairy Nanoparticle. It is of interest to investigate the average number of grafted polymer chains, i.e., "hairs", per nanoparticle (N_{hair}). This value was determined by the number of initiating sites originally present in each latex particle ($N_{0,EBiB}$), the fraction of polymers incorporated in the nanoparticle ($A_{particle}$), and the initiation efficiencies in the first (IE_{first}) and second steps (IE_{second}) of the continuous copolymerization, i.e., microemulsion and seeded emulsion ATRP. In order to achieve at least a semiquantitative idea about the initiation efficiencies during the nanogel core formation and the following "grafting from" steps, hairy nanoparticles with degradable nanogel cores were prepared by using a reductively degradable disulfide-bearing cross-linker SS (see Scheme 1 for chemical structure) during the microemulsion ATRP step. Following the same experimental procedures detailed above, 200 equiv of *n*BA (vs the initial amount of EBiB) was added to the reaction system, and the temperature was increased to 80 °C. The polymerization was stopped at 20 h by exposing the reaction to air with the conversion of *n*BA around $conv_{nBA} = 31\%$. The emulsion latex was dried and redispersed in THF for further analysis.

The degradation was carried out by adding the reducing agent, Bu_3P, to the THF dispersion of nanogel cores as well as to a dispersion of hairy nanoparticles. Figure 3 shows the GPC curves of the nanogel core, hairy nanoparticle, and the cleaved products. After degradation of the nanogel core, only one elution peak with lower molecular weight was seen in the GPC trace, representing the cleaved product P(MMA−S), where S represents the $CH_2-(CH_3)C(COOCH_2CH_2SH)$ unit. According to GPC measurement, the degradation of the nanogel cores resulted in the formation of linear polymers, which had an apparent molecular weight $M_{n,RI} = 3.1 \times 10^3$ g/mol based on linear PS standards. Given the essentially complete conversion of double bonds during the core formation, the theoretical molecular weight of PMMA primary chains (if 100% initiation efficiency was achieved) was estimated to be $M_{n,theor} = MW_{EBiB} + 18 \times MW_{MMA} + 2 \times MW_{SS} = 195.05 + 18 \times 100.12 + 2 \times 290.4 \approx 2.6 \times 10^3$ g/mol. Thus, the initiation efficiency in the microemulsion ATRP step was ca. $IE_{first} = 2.6 \times 10^3/3.1 \times 10^3 \approx 84\%$.

After extension of P*n*BA chains from the cross-linked PMMA nanogel core, the polymer product showed two elution peaks, representing the hairy nanoparticles and a fraction of free linear chains (Figure 3). The area fraction of hairy nanoparticles was ca. $A_{particle} = 70\%$, determined by multipeak splitting of the GPC curve using Gaussian function. The elution peak of hairy nanoparticles became undetectable after degradation and the cleaved product showed a GPC trace overlapped with that of the linear polymers formed during the preparation of hairy nanoparticles, indicating a close-to-complete degradation of the hairy nanoparticles to linear polymers, P(MMA−S)-*b*-P*n*BA. The GPC trace of P(MMA−S)-*b*-P*n*BA chains was well separated from that of the cleaved product form PMMA nanogel core, indicating a high initiation efficiency in the second emulsion ATRP step, i.e., $IE_{second} \sim 1$.

Since the theoretical number of EBiB in each nanogel core was around $N_{0,EBiB} = 3.8 \times 10^3$, based on the size of nanogel ($D_h = 31$ nm) and the concentration of EBiB in monomer, the number-average number of grafted chains, "hairs", per hairy nanoparticle could be calculated as $N_{hair} = N_{0,EBiB} \times IE_{first} \times A_{particle} \times IE_{second} = 3.8 \times 10^3 \times 84\% \times 70\% \times 100\% \approx 2.3$

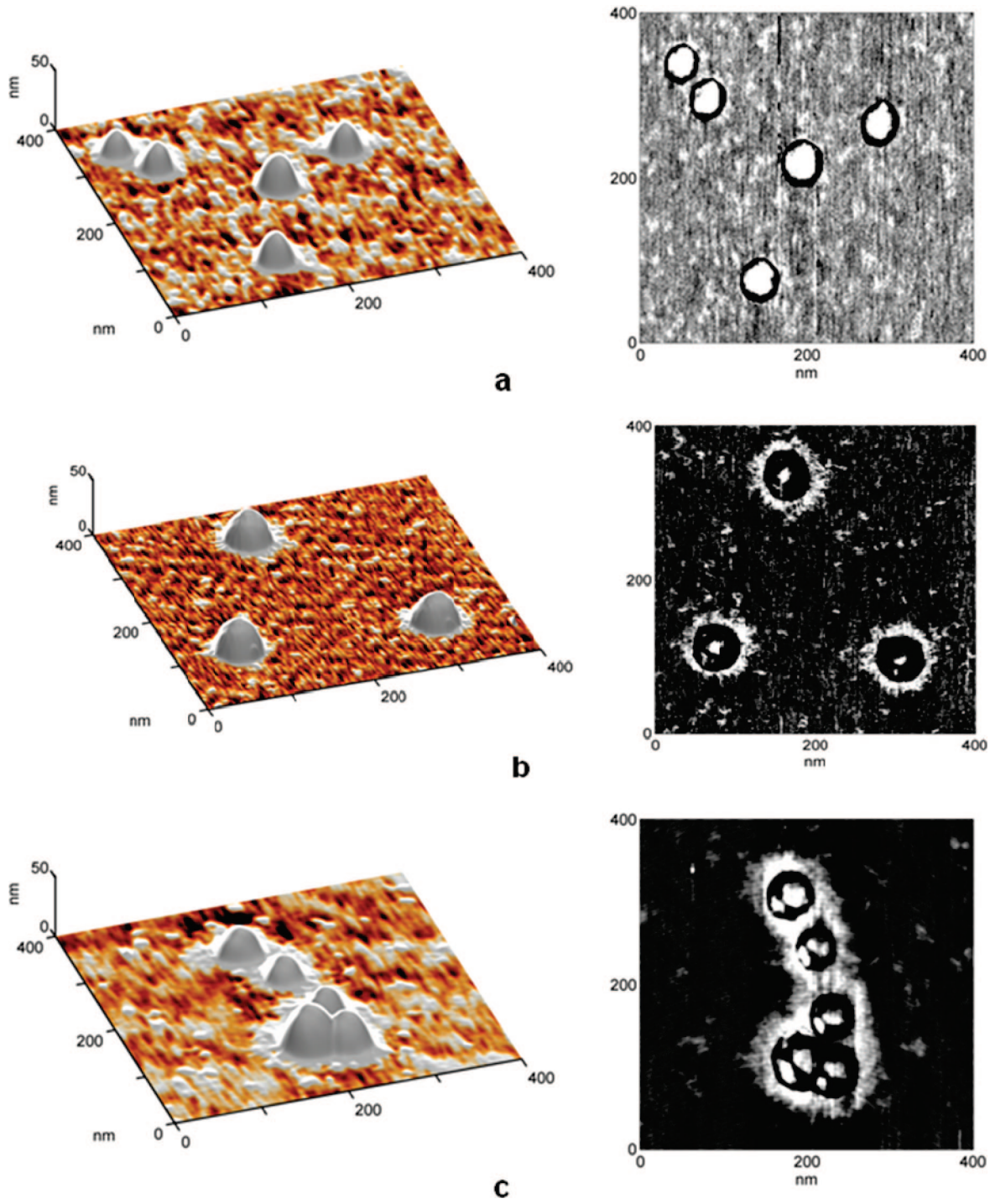

Figure 4. 3D (left) and phase (right) tapping mode AFM images of hairy nanoparticles with permanent cross-linker EGDMA produced with different polymerization times *t*: (a) $t = 1.6$ h, coronas narrower than 10 nm; (b) $t = 3.1$ h, average corona width 17 nm; (c) $t = 6.1$ h, average corona width 30 nm. The synthesis conditions and the results are listed in Tables 1 and 2. The images were taken from particle dispersions in chloroform (0.2 mg/mL) spin-coated onto mica surface.

$\times 10^3$. If all of the grafted P*n*BA chains grew from the surface of the cross-linked PMMA core ($D_h = 31$ nm), the value of $N_{hair} = 2.3 \times 10^3$ corresponds to a maximum grafting density of P*n*BA, ca. 0.75 chains/nm^2, which is comparable to a typical grafting density obtained by grafting polymer chains from silica nanoparticles.[42] The actual grafting density of P*n*BA chains on the core surface was less than 0.75 chains/nm^2 because a fraction of the grafted chains were determined to grow from the initiating sites inside the PMMA cores, which will be discussed later.

After degradation of the hairy nanoparticles by using Bu_3P, the degraded polymer P(MMA−S)-*b*-P*n*BA showed an apparent molecular weight $M_{n,RI} = 1.30 \times 10^4$ g/mol based on linear PSt standards. Since the apparent molecular weight of P(MMA−S) primary chains was around $M_{n,RI} = 3.1 \times 10^3$ g/mol, the apparent molecular weight of the second P*n*BA block could be estimated as $1.30 \times 10^4 - 3.1 \times 10^3 = 9.9 \times 10^3$ g/mol. On the other hand, the theoretical molecular weight of the P*n*BA block could be calcuated based on the conversion of *n*BA at 20 h and the initiation efficiency of the microemulsion ATRP step $IE_{first} = 84\%$: $M_{n,theor}(PnBA) = (DP_{nBA,target} \times MW_{nBA} \times conv_{nBA})/IE_{first} = (200 \times 128.17 \times 0.31)/0.84 \approx 9.5 \times 10^3$

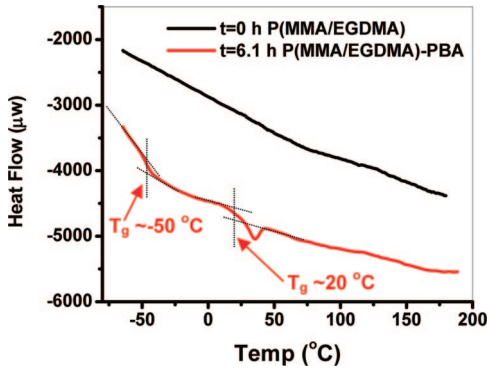

Figure 5. DSC thermograms of the cross-linked PMMA nanogel cores and the hairy nanoparticles PMMA−P*n*BA. The heating rate was 10 °C/min during the DSC analysis under a nitrogen atmosphere over a temperature range of −60 to 180 °C. The second heating cycle was recorded. The synthesis conditions of the nanogel and the hairy nanoparticles are listed in Table 1.

g/mol. This result is in agreement with the value determined based on GPC analysis.

Visualization of Hairy Nanoparticles by AFM. In recent years, tapping mode AFM has been shown to be particularly useful in validating the structure of complex nanoobjects, such as polymer brushes,[43] hairy nanoparticles[11] and polymer-grafted carbon nanotubes,[44] by facilitating the direct visualization of coronas formed by polymer "hair" chains spreading on the suitable substrate (mostly mica). As shown in Figure 4, these characteristic structures were also observed in the present study, when the nanoparticles were deposited on mica. In 3D height images (Figure 4, left) the P*n*BA coronas were manifested as stringy chains extending from bulky PMMA cores onto the mica substrate. In phase images (Figure 4, right) they appeared as brighter fringed rings surrounding nanoparticle cores (for discussion of phase contrast in tapping mode AFM images of hairy nanoobjects see, e.g., ref42). Whereas for the polymerization time of 1.6 h (Figure 4a) the P*n*BA coronas were still barely distinguishable, their width markedly increased for the polymerization times of 3.1 h (Figure 4b) and 6.1 h (Figure 4c) to reach respectively ca. 17 and 30 nm (measurements based on phase images). In addition to hairy nanoparticles, all AFM images revealed also the presence of free polymer chains on the mica surface, corresponding to the unbound polymer fraction manifested as peaks at higher elution volume in Figure 2.

Assuming all *trans* conformation of C−C backbones on the mica substrate, the observed corona widths of 17 and 30 nm provide the lower bound estimates of the degree of polymerization of the longest P*n*BA chains equal to DP = 68 and 120. Considering that the amount of *n*BA added was 200 times the amount of EBiB initiator and that the conversions of *n*BA after 3.1 and 6.1 h were 12% and 20%, the overall initiation efficiency of the polymerization was calculated to be ca. 0.35. This value is lower than the previously determined value $IE_{overall} = IE_{first} \times IE_{second} = 0.84$, estimated from the GPC analysis of the cleaved products from hairy nanoparticles containing disulfide cross-link. Since the AFM characterization mostly provides information on the longest hairy chains grafted on the substrate,[45,46] the initiation efficiency calculated by AFM analysis was very likely to be underestimated.

Thermal Properties of Hairy Nanoparticles. It is worth noting that some alkyl bromide initiating sites encapsulated inside the PMMA nanogel cores were capable of chain extension as long as they were in contact with catalysts and monomers. Thus, the growth of P*n*BA chains could occur not only on the surface of the cross-linked PMMA core but also inside the PMMA core. Evidence for polymerization inside the nanogel was obtained during DSC analysis of the hairy nanoparticles (Figure 5). Prior to chain extension (sample at $t = 0$ h), the highly cross-linked PMMA nanogel displayed no clear T_g in the temperature range (−60 to 180 °C). In contrast, the sample taken at $t = 6.1$ h, corresponding to a hairy nanoparticle containing 68 wt % of P*n*BA hairs, showed two T_gs. The first T_g appearing at −50 °C corresponded to that of P*n*BA hairs, while the second one appearing at 20 °C is much lower than that of PMMA homopolymer. This second T_g peak is possibly due to the growth of some P*n*BA chains inside the nanogel core, which could not efficiently phase separate from the cross-linked PMMA core and resulted in a compromised T_g between that of PMMA and that of P*n*BA. As discussed above, the growth of some P*n*BA chains inside the PMMA core could result in a lower grafting density of P*n*BA chains on the core surface than the calculated value, e.g., grafting density < 0.75 chains/nm^2.

Conclusions

An efficient one-pot synthesis of well-defined hairy nanoparticles was developed by applying ATRP to an emulsion medium. The first step was a microemulsion ATRP of a monomer, MMA, and a cross-linker, EGDMA, leading to the uniform cross-linked nanogels ($D_h \sim 31$ nm). Addition of a second monovinyl monomer, *n*BA, to the microemulsion converted the polymerization into a seeded emulsion system. P*n*BA successfully grew from the retained initiating functionalities in the nanogels, forming hairy nanoparticles in situ. The application of emulsion polymerization procedures confined the growth of each hairy nanoparticle in one latex, resulting in hairy nanoparticles with a uniform size distribution, as indicated by DLS analysis (coefficient of variation <0.3). When a reductively degradable cross-linker was used in the first step, the obtained PMMA nanogel and PMMA−P*n*BA hairy nanoparticles could be degraded. The GPC analyses of the cleaved products provided a means to determine the number of grafted polymer chains per hairy nanoparticle as $N_{hair} \sim 2.3 \times 10^3$, corresponding to a maximum grafting density of 0.75 chains/nm^2 on the surface of nanogel. Direct visualization of the hairy particles by AFM provided additional evidence for a uniform particle synthesis. DSC measurement of the hairy nanoparticles showed two T_gs (−50 and 20 °C), corresponding to P*n*BA hairs and the non-phase-separated PMMA/P*n*BA blends in the core segments, which were the product by growth of P*n*BA hairs on nanogel surface and inside the nanogel core. All these results proved the development of an alternative and convenient method for synthesis of hairy nanoparticles with controlled size and hair density.

Acknowledgment. The financial support from NSF Grant DMR 05-49353 and the CRP Consortium at Carnegie Mellon University is appreciated. K. Min acknowledges the support from the Bayer Fellowship.

References and Notes

(1) Kawaguchi, H.; Isono, Y.; Tsuji, S. *Macromol. Symp.* **2002**, *179*, 75–87.
(2) Kawaguchi, H. *Prog. Polym. Sci.* **2000**, *25*, 1171–1210.
(3) Li, D. J.; Sheng, X.; Zhao, B. *J. Am. Chem. Soc.* **2005**, *127*, 6248–6256.
(4) Pichot, C. *Curr. Opin. Colloid Interface Sci.* **2004**, *9*, 213–221.
(5) Yezek, L.; Schartl, W.; Chen, Y. M.; Gohr, K.; Schmidt, M. *Macromolecules* **2003**, *36*, 4226–4235.
(6) Klos, J.; Pakula, T. *J. Chem. Phys.* **2003**, *118*, 7682–7689.
(7) Min, K.; Hu, J.; Wang, C.; Elaissari, A. *J. Polym. Sci., Part A: Polym. Chem.* **2002**, *40*, 892–900.
(8) Bian, K.; Cunningham, M. F. *Polymer* **2006**, *47*, 5744–5753.
(9) D'Agosto, F.; Charreyre, M.-T.; Pichot, C.; Gilbert, R. G. *J. Polym. Sci., Part A: Polym. Chem.* **2003**, *41*, 1188–1195.
(10) Amamoto, Y.; Higaki, Y.; Matsuda, Y.; Otsuka, H.; Takahara, A. *J. Am. Chem. Soc.* **2007**, *129*, 13298.

(11) Pyun, J.; Kowalewski, T.; Matyjaszewski, K. *Macromol. Rapid Commun.* **2003**, *24*, 1043–1059.
(12) Matyjaszewski, K., Davis, T. P., Eds.; *Handbook of Radical Polymerization*; Wiley: Hoboken, NJ, 2002.
(13) Braunecker, W. A.; Matyjaszewski, K. *Prog. Polym. Sci.* **2007**, *32*, 93–146.
(14) Pyun, J.; Matyjaszewski, K.; Kowalewski, T.; Savin, D.; Patterson, G.; Kickelbick, G.; Huesing, N. *J. Am. Chem. Soc.* **2001**, *123*, 9445–9446.
(15) Liu, T. Q.; Jia, S.; Kowalewski, T.; Matyjaszewski, K.; Casado-Portilla, R.; Belmont, J. *Langmuir* **2003**, *19*, 6342–6345.
(16) Tsuji, S.; Kawaguchi, H. *Langmuir* **2004**, *20*, 2449–2455.
(17) Bombalski, L.; Min, K.; Dong, H.; Tang, C.; Matyjaszewski, K. *Macromolecules* **2007**, *40*, 7429–7432.
(18) Esteves, A. C. C.; Bombalski, L.; Trindade, T.; Matyjaszewski, K.; Barros-Timmons, A. *Small* **2007**, *3*, 1230–1236.
(19) Dong, H.; Zhu, M.; Yoon, J. A.; Gao, H.; Jin, R.; Matyjaszewski, K. *J. Am. Chem. Soc.* **2008**, *130*, 12852–12853.
(20) Oh, J. K.; Drumright, R.; Siegwart, D. J.; Matyjaszewski, K. *Prog. Polym. Sci.* **2008**, *33*, 448–477.
(21) Taton, D.; Baussard, J.-F.; Dupayage, L.; Poly, J.; Gnanou, Y.; Ponsinet, V.; Destarac, M.; Mignaud, C.; Pitois, C. *Chem. Commun.* **2006**, 1953–1955.
(22) Delaittre, G.; Save, M.; Charleux, B. *Macromol. Rapid Commun.* **2007**, *28*, 1528–1533.
(23) Gao, H.; Matyjaszewski, K. *Macromolecules* **2008**, *41*, 1118–1125.
(24) Gao, H.; Li, W.; Matyjaszewski, K. *Macromolecules* **2008**, *41*, 2335–2340.
(25) Gilbert, R. G. *Emulsion Polymerization*; Academic Press: London, 1995.
(26) Lovell, P. A., El-Aasser Mohamed S., Ed.; *Emulsion Polymerization and Emulsion Polymers*; John Wiley & Sons: New York, 1997.
(27) Wang, J.-S.; Matyjaszewski, K. *J. Am. Chem. Soc.* **1995**, *117*, 5614–5615.
(28) Matyjaszewski, K.; Xia, J. H. *Chem. Rev.* **2001**, *101*, 2921–2990.
(29) Kamigaito, M.; Ando, T.; Sawamoto, M. *Chem. Rev.* **2001**, *101*, 3689.
(30) Tsarevsky, N. V.; Matyjaszewski, K. *Chem. Rev.* **2007**, *107*, 2270–2299.
(31) Qiu, J.; Gaynor, S. G.; Matyjaszewski, K. *Macromolecules* **1999**, *32*, 2872–2875.
(32) Qiu, J.; Charleux, B.; Matyjaszewski, K. *Prog. Polym. Sci.* **2001**, *26*, 2083–2134.
(33) Min, K.; Gao, H.; Matyjaszewski, K. *J. Am. Chem. Soc.* **2005**, *127*, 3825–3830.
(34) Jakubowski, W.; Matyjaszewski, K. *Macromolecules* **2005**, *38*, 4139–4146.
(35) Min, K.; Matyjaszewski, K. *Macromolecules* **2005**, *38*, 8131–8134.
(36) Xia, J.; Matyjaszewski, K. *Macromolecules* **1999**, *32*, 2434–2437.
(37) Gao, H.; Tsarevsky, N. V.; Matyjaszewski, K. *Macromolecules* **2005**, *38*, 5995.
(38) Min, K.; Gao, H.; Matyjaszewski, K. *J. Am. Chem. Soc.* **2006**, *128*, 10521–10526.
(39) Siegwart, D. J.; Oh, J. K.; Gao, H.; Bencherif, S. A.; Perineau, F.; Bohaty, A. K.; Hollinger, J. O.; Matyjaszewski, K. *Macromol. Chem. Phys.* **2008**, *209*, 2179–2193.
(40) Gao, H.; Matyjaszewski, K. *Macromolecules* **2006**, *39*, 3154–3160.
(41) Michielsen, S. In *Polymer Handbook*, 4th ed.; Brandrup, J., Immergut, E. H., Grulke, E. A., Eds.; Wiley: New York, 1999.
(42) Pyun, J.; Jia, S. J.; Kowalewski, T.; Patterson, G. D.; Matyjaszewski, K. *Macromolecules* **2003**, *36*, 5094–5104.
(43) Sheiko, S. S.; Moller, M. *Chem. Rev.* **2001**, *101*, 4099–4123.
(44) Wu, W.; Tsarevsky, N. V.; Hudson, J. L.; Tour, J. M.; Matyjaszewski, K.; Kowalewski, T. *Small* **2007**, *3*, 1803–1810.
(45) Sheiko, S. S.; Prokhorova, S. A.; Beers, K. L.; Matyjaszewski, K.; Potemkin, I. I.; Khokhlov, A. R.; Moller, M. *Macromolecules* **2001**, *34*, 8354–8360.
(46) Sheiko, S. S.; Sumerlin, B. S.; Matyjaszewski, K. *Prog. Polym. Sci.* **2008**, *33*, 759–785.

MA8026244